Shapes of Atomic Nuclei: Recent Experiments and Open Questions

Dimiter L. Balabanski[1,2]

[1] INRNE, Bulgarian Academy of Sciences, BG-1784 Sofia,Bulgaria
[2] Universitá di Camerino and INFN-Perugia, 62032 Camerino, Italy

Abstract. This paper reports on recent experimental studies of quadrupole moments and reduced transition probabilities in atomic nuclei. First, based on the deduced $B(E2)$ transition strength from a measurement of lifetimes, ^{128}Ce is suggested as a benchmark for the X(5) critical point symmetry in the mass $A \approx 130$ region. Next, a quadrupole moment measurement of the $\frac{29}{2}^-$ bandhead of a magnetic rotational band in ^{193}Pb and a measurement of lifetimes in the band are presented and compared to calculations within the framework of the tilted-axis cranking model. Last, the measured quadrupole moment of the five-qusiparticle $\frac{35}{2}^+$ high-K isomer in ^{179}W is discussed. In all cases the experimental observations provide important information for the understanding of the evolution of the shape for different excitations and, due to the improved sensitivity of the experiments, pose new questions related to different shape-driving effects.

1 Introduction

Since the discovery of non-zero electric quadrupole moments, which is direct proof for breaking of the spherical symmetry, shape became a major concept in physics of atomic nuclei. Three different shape-related phenomena are reported: Shape/phase transitions and deformations of magnetic bands and of high-K isomers.

The study of phase transitions in mesoscopic systems, such as nuclei, molecules or atomic clusters is a topic of interest in current physics research [1]. Here an example is provided from a recent lifetime measurement in ^{128}Ce. The deduced $B(E2)$ transition strengths for the yrast sequence together with the energies of the levels within the ground-state (*gs*) band of ^{128}Ce are in agreement with the predicted values for the X(5) critical point symmetry, which defines a phase/shape transition between a spherical vibrator and an axially symmetric rotor. Hence this nucleus is suggested as a benchmark for X(5) symmetry [2].

The quadrupole moment measurements for the $\frac{29}{2}^-$ bandhead of a magnetic band in ^{193}Pb [3] and for the $\frac{35}{2}^+$ high-K isomer in ^{179}W [4] are presented and different deformation-driving effects are discussed. In the former case also lifetimes in the band were measured [5]. This is the first complete set of experimental observables in a magnetic band, which provides test ground for the models aiming at the description of such excitations. In the latter case it was shown that the high-K state is less deformed than the ground state.

2 Shape/Phase Transitions in Nuclei: The Case of ^{128}Ce

Critical-point symmetries [6, 7], describing nuclei at points of phase/shape transitions between the limiting symmetries of IBM-1 [8], attract considerable attention, since they yield parameter independent solutions (up to scale factors) which are found to be in good agreement with experiment [9, 10]. The above descriptions are solutions of the differential equations associated with the Bohr Hamiltonian [11]. A solution of this equation that is appropriate to the critical point of the spherical, U(5), to axially deformed, SU(3), transition, is called X(5) [7]. This solution is not an exact solution of the Bohr Hamiltonian and its derivation involves certain approximations, and an open problem that remains is how to treat simultaneously the β and γ excitations.

On the basis of the energies of the levels in the *gs* band ($R_{4/2} = 2.93$), this nucleus was suggested as a candidate for the X(5) symmetry. Here we report lifetime measurements of excited states in the ground state (*gs*) band of ^{128}Ce.

2.1 Experiment

The experiment was performed at the Wright Nuclear Structure Laboratory of Yale University. Excited states in ^{128}Ce were populated in the ^{100}Mo(^{32}Si,4n) reaction at 120 MeV and the nuclear γ decay was measured with an array of eight Clover detectors positioned at forward and backward angles. Events were collected when at least two γ rays were detected by two independent Clover detectors. Lifetimes of excited states in ^{128}Ce were measured using the recoil-distance Doppler-shift (RDDS) and Doppler-shift attenuation (DSAM) methods. For the RDDS experiment the Yale plunger device was used. The target was a ≈ 1 mg/cm^2 thick self-supporting ^{100}Mo foil and a 10 mg/cm^2 Au foil was used as stopper for the recoils. The mean recoil velocity was $v/c = 1.9\%$. Measurements at four target-to-stopper distances were carried out.

For the RDDS measurement, $\gamma\gamma$ coincidence spectra were obtained for each target-to-stopper distance by gating on the Doppler-shifted components of the transitions in the *gs* band. The peak intensities of both, the shifted (S) and the unshifted (U) components of all transitions of interest were determined at each target-to-stopper position in order to analyze the data by the Differential Decay Curve Method (DDCM) [12] and derive the corresponding decay curves. According to the DDCM, if transition B is populating a level of interest, and it is depopulated via transition A, in the special case of gating on the Doppler-shifted component of the direct feeding transition, the mean lifetime τ can be derived for each target-to-stopper distance by applying the following equation:

$$\tau(x) = \frac{1}{v} \cdot \frac{I_{SU}^{BA}(x)}{\frac{d}{dx} I_{SS}^{BA}(x)}, \tag{1}$$

where v is the recoil velocity. The quantities $I_{SU}^{BA}(x)$and $I_{SS}^{BA}(x)$ denote the normalized, measured intensities of the shifted (S) and unshifted (U) components of

the depopulating γ transition A in coincidence with the shifted (S) component of a populating γ transition B.

The target for the DSAM measurement consisted of 500 μg/cm^2 ^{100}Mo evaporated on a 9 mg/cm^2 Au foil. For the data analysis we performed a Monte Carlo simulation of the slowing-down histories of the recoils [13]. The analysis of the line shapes was carried out following the DDCM procedure for DSAM data [14,15]. The lifetimes of the 8_1^+ and 10_1^+ levels of the *gs* band were deduced from these data. The lifetime of the 8_1^+ state (albeit the large uncertainty) in excellent agreement with the value obtained from the RDDS measurement.

2.2 Results and Discussion

Lifetimes (and the corresponding $B(E2)$ reduced transition probabilities) were derived from the data for the $4_1^+, 6_1^+, 8_1^+$ and 10_1^+ levels in ^{128}Ce and a limit was set for the 4_2^+ level. The results are in agreement with literature values for the 4_1^+ [16, 17] and 8_1^+ [16,18] levels, while the obtained lifetime of the 10_1^+ state, $\tau = 0.45(10)$ ps, is much smaller compared to the values published previously [16, 18].

After ^{152}Sm was suggested as a X(5) nucleus [10], attempts to find examples in other mass regions were made. In the mass $A \approx 100$ region ^{104}Mo was considered a X(5) candidate, based on the energies of the levels in the *gs* band [19]. The lifetime measurement and the derived $B(E2)$ reduced transition probabilities in this case turned out to follow the rotor limit [20]. In ^{128}Ce the ratio of the energies in the *gs* band $R_{4/2} = 2.93$ is close to the X(5) value, $R_{4/2}^{X(5)} = 2.91$. The energy of the first excited 0_2^+ state is also close to the reference value in X(5): $R_{0/2} = E(0_2^+)/E(2_1^+) = 5.08$, compared to the X(5) value $R_{0/2}^{X(5)} = 5.64$. Yrast energies and $B(E2)$ values deduced from this experiment for the *gs* band in ^{128}Ce are presented in Figure 1. The agreement with the X(5) limit in both cases is excellent.

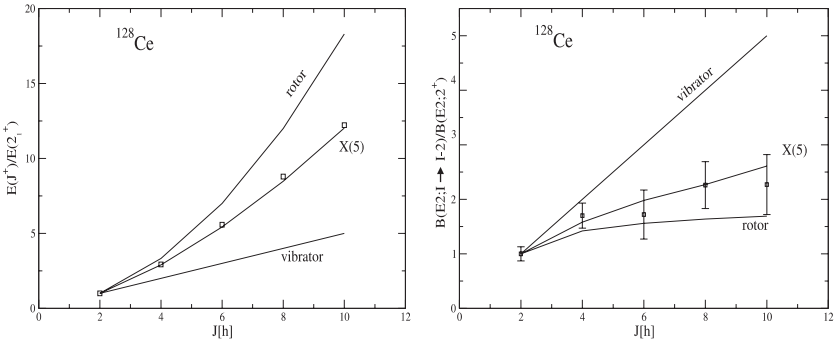

Figure **1.** Left: Excitation energy ratios $R_i = E_i/E_{2^+}, i = 4, 6, 8, 10$ in ^{128}Ce and the corresponding X(5) predictions. Right: Relative $B(E2)$ values measured in the *gs* band in ^{128}Ce compared to the corresponding X(5) prediction.

It is interesting to note that all three nuclei, ^{152}Sm, ^{104}Mo and ^{128}Ce are mirror nuclei in the N_pN_n scheme with $N_pN_n = 96$. They have either eight (or twelve) valence protons (or proton holes) and twelve (or eight) neutrons (or neutron holes). In the cases of ^{152}Sm and ^{128}Ce, both of which follow the X(5) limit, the number of protons is below mid-shell, which poses the question on the role of the particle states for critical point behavior.

In conclusion, the derived $B(E2)$ reduced transition probabilities indicate that ^{128}Ce lies close to the U(5)-SU(3) phase shape transition. The excitation energies of the γ band are also in agreement with the X(5) values [6, 19, 21]. It is necessary to investigate the transition strengths in and out of the β and γ bands in ^{128}Ce in order to establish it firmly as a X(5) critical point nucleus.

3 Magnetic Rotation in the Lead Region: The Case of ^{193}Pb

In recent years collective excitations, such as "magnetic rotation", which is observed at closed-shell nuclei, have been studied intensively. These excitations are suggested to result from the perpendicular coupling of valence particles and holes [31].

The microscopic world imposes a severe restriction on rotational motion: the spherical symmetry must be broken for a quantal system. Thus, the rotation of an atomic nucleus is associated with the presence of a large electric quadrupole moment, i.e. with the breaking of the spherical symmetry of the charge distribution. As a result, sequences of enhanced electric quadrupole ($E2$) transitions connecting $\Delta I = 2$ levels are observed in experiment; I denotes the nuclear spin. Rotational-like sequences of enhanced magnetic dipole ($M1$) transitions between $\Delta I = 1$ states, known as magnetic rotational bands, have been observed for closed-shell nuclei; see [22, 23] for reviews. Their appearance is understood as due to the coupling of high-j particle and hole excitations which create states for which the rotational symmetry with respect to the angular momentum vector is broken. The associated total magnetic dipole moment is not oriented along the direction of the angular momentum. This specifies an orientation which is needed for the formation of rotational-like sequences. It is well known that the $M1$ transition probability depends on the perpendicular component of the magnetic moment vector with respect to the angular momentum direction, while the static magnetic moment depends on its parallel component [24] and, therefore, a large component of the magnetic moment perpendicular to the angular momentum should exist for these excitations. Angular momentum along the $M1$ bands is generated by the step-by-step alignment of the particle and hole spins into the direction of the total angular momentum, which resembles the closing of a pair of shears and is referred to as "shears mechanism".

For the $Z = 82$ Lead nuclei more than sixty magnetic rotational bands have been established [25]. It is well known that different shapes co-exist for the Pb nuclei. For the $\nu i_{13/2}^{-n}$ states small quadrupole moments have been measured and these are understood to polarize the core towards small prolate deformations [26]. The spectroscopic quadrupole moments of the proton particle-hole (2p2h) excitations across the $Z = 82$ shell, which are observed as 11^- isomers in the mid-shell Pb nuclei, take

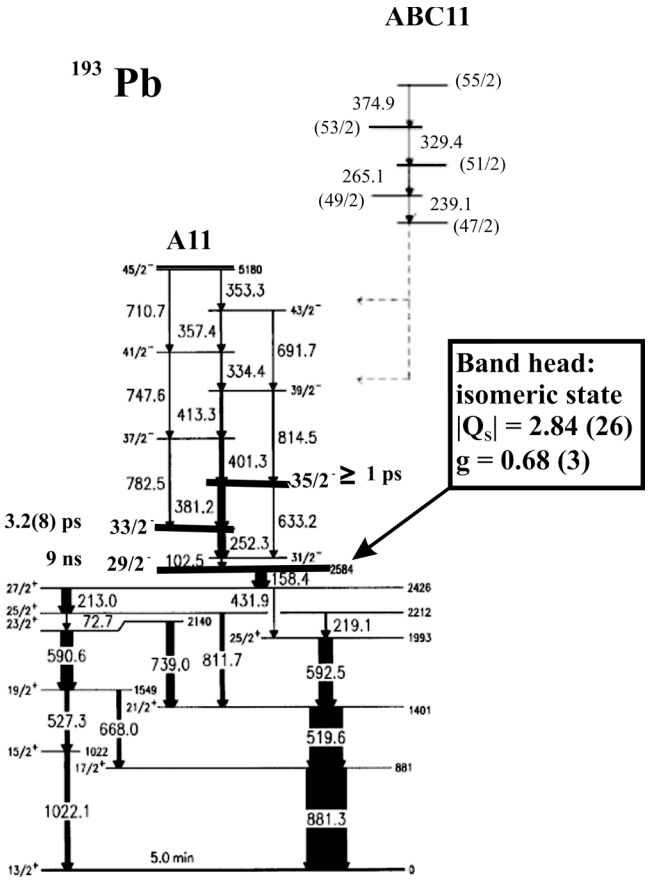

Figure **2.** A partial level scheme of ^{193}Pb, revealing the transitions and the γ decay of the $A11$ band.

large values and correspond to moderate oblate deformations, $\beta_2 \approx 0.12-0.18$ [27]. The band heads of the magnetic bands in the Pb nuclei result from the coupling of the above excitations. The lowest lying (yrast) magnetic band in odd-A isotopes is built on the $\pi i_{13/2} \otimes 11^-$ configuration, further denoted as the $A11$ band. A partial level scheme, revealing the transitions of in the $A11$ band in ^{193}Pb and the decay of band head, which is $I^\pi = \frac{29}{2}^-$ isomeric state ($E_{ex} = 2584$ keV, $T_{1/2} = 9.4$ ns) is presented in Figure 2. The spin and parity of the band head have been assigned on the basis of DCO analysis of the transitions below the isomer [28, 29]. The configuration of the band head is supported by a g-factor measurement, assuming a perpendicular coupling of the valence particles [30].

Recently, the quadrupole moment of the $\frac{29}{2}^-$ isomer was measured [3]. The experiment was carried out at the Laboratori Nazionali di Legnaro and the isomer was populated in the ^{170}Er(^{28}Si,5n) reaction at 149 MeV. The quadrupole interaction

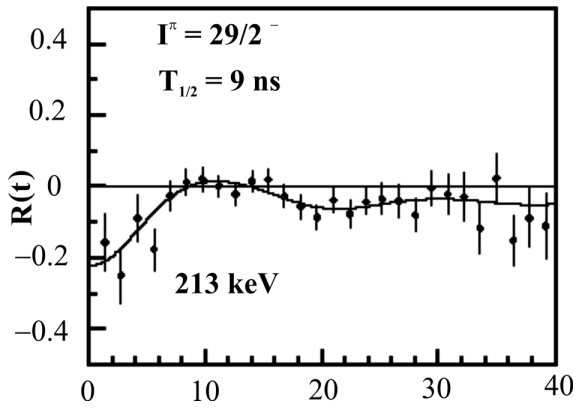

Figure **3.** TDPAD spectra for decay γ rays of the $29/2^{+}$ isomer in ^{193}Pb showing the quadrupole interaction in a solid Hg host at $T = 170(1)$ K.

of ^{193}Pb in solid Hg was studied by applying the time-differential perturbed angular distribution (TDPAD) technique. The Hg host was chosen because it provides a large electric-field gradient (EFG): $V_{ZZ} = 17.4(9) \cdot 10^{21}$ V/m^2 at $T = 170$ K, which results in a strong interaction on the short time scale defined by the isomer lifetime. Sample experimental TDPAD curves are displayed in Figure 3. The measured static quadrupole moment $|Q_s| = 2.84(26)\ e$b [3] indicates that the 2p2h proton excitations determine the deformation of this state.

Extensive set of calculations have been done within the framework of the tilted-axis cranking (TAC) model [31]. A local parametrization of the model for the Pb nuclei has been obtained reproducing the quadrupole moments for the $\nu i_{13/2}^{-n}$ states, using the usual $A^{-5/3}$ mass-scaling factor [32]. Within this parametrization, the measured quadrupole moments of the 11^{-} states in ^{192,194,196}Pb are reproduced reasonably well, and the calculation yields $|Q_s| = -2.85\ e$b for the $A11$ band head, in a perfect agreement with the experiment.

A next step was to study the transition strength within the $A11$ band. This experiment was carried out also at the Laboratori Nazionali di Legnaro, using the GASP spectrometer and the Köln plunger device. Excited states in the $A11$ band were populated in the same ^{170}Er(^{28}Si,5n) reaction at 149 MeV. During the experiment a RDDM (in order to approach the lifetimes at the bottom of the $A11$ band) and DSAM measurements were done. Here we report results from the analysis of the RDDM data. Spectra were recorded for nine different distances, in the range from 0.1 μm to 257.1 μ and triple $\gamma\gamma\gamma$-coincidence events were recorded. For each distance the events were sorted into $\gamma\gamma$-coincidence matrices with γ rays detected in a given detector ring placed on one axis and γ rays detected elsewhere in the array along the second axis of the matrix. In order to extract the lifetimes of interest, the DDCM method [12] was used. The results are presented in Table 1.

The matrix element for the 633.2-keV transition has been extracted using the known branching ratio [28, 29]. From the deduced $B(E2)$ strength one can set an

Table **1.** Lifetimes of excited states in the $A11$ band in ^{193}Pb.

E_{ex} (keV)	E_γ (keV)	$I^\pi_{in} \rightarrow I^\pi_f$	σL	τ (ps)	B(σL)
2939	252.3	$33/2^- \rightarrow 31/2^-$	M1	3.2(8)	1.1(2) μ_N^2
3220	381.2	$35/2^- \rightarrow 33/2^-$	M1	≤ 1	$\geq 1.4\ \mu_N^2$
3220	633.2	$35/2^- \rightarrow 33/2^-$	E2	–	$\geq 0.1\ e$b

upper limit for the intrinsic quadrupole moment $Q_0 \geq 1.69\ e$b, which in turn provides a limit for the deformation $\beta_2 \geq 0.056$.

In summary, the measured lifetimes in the $A11$ magnetic band in ^{193}Pb [5] together with the previously measured DCO and branching ratios for the transitions in the band [28, 29], as well as the g factor [30] and the quadrupole moment [3] of the band head, provide a complete set of experimental observables for such an excitation in atomic nuclei which can be used for a stringent test of the theoretical models aiming at the description of magnetic rotation. The results from TAC calculations for the $B(M1)$ strength, adjusted to the measured quadrupole moments in the Pb nuclei, are in a reasonable agreement with the experimental data [32]. It should be noted, however, that the $B(M1)/B(E2)$ ratios cannot be reproduced well within this parameterization.

4 Shapes of K Isomers: The Case of ^{179}W

Several distinct types of isomers are known in atomic nuclei: shape isomers, spin traps and K isomers [33]. Shape isomers arise when a metastable state decays to a state with a different shape and it is difficult to rearrange the nuclear configuration. Spin traps appear due to the spin-selection rules. The third type of isomer, known as a "K trap" is caused by the necessity ot change the spin orientation relative to an axis of symmetry. K is a quantum number that represents the projection of the total spin along the symmetry axis of the nuclear potential. Therefore, these type of isomers are expected to arise only in axially-symmetric, well-deformed nuclei, for which K should be a good quantum number. A number of such states have been established in the Hf-W-Os region.

Here the following question is addressed: Is there a difference between the deformation of the nuclei in their ground states and in their high-seniority multi-quasiparticle excitations. Its importance is related to quenching of pairing in atomic nuclei. Prior our experiments [4] only the quadrupole moments of the high-K isomers in ^{182}Os ($K^\pi = 25^+$) [34], ^{178}Hf ($K^\pi = 16^+$) [35, 36], and ^{177}Lu ($K^\pi = \frac{23}{2}^-$) [37] were measured. Recently Billowes *et al.* established a programme to investigate mean charge radii of isomeric states with collinear laser spectroscopy at the IGISOL in Jyvaskyla, Finland [38].

The ^{170}Er(^{13}C,4n)^{179}W reaction at 63 MeV was used to populate the $\frac{35}{2}^+$ isomer. A thin self-supporting, 98% enriched, 500 μg/cm^2 ^{170}Er target was used in

experiment. The recoiling out isomers were in-beam implanted into a thick policrystaline Tl foil which served as a host and a beam stopper. The experiments were performed at the CYCLONE cyclotron at Louvain-la-Neuve, Belgium, using the level-mixing spectroscopy (LEMS) technique [39,40]. The experimental set-up consisted of 4.4 T superconducting split-coil magnet, a target holder, allowing precise temperature control at the targer position in the interval $4 - 600$ K, and four Ge detectors, positioned at 0° and 90° with respect to the beam axis, which monitor the target through the holes of the magnet.

The choice of the host material is crucial for a LEMS experiment, since the measured quadrupole frequency depends on the nuclear quadrupole moment and the EFG of the material as $\nu_Q = \frac{e}{h} Q_s V_{ZZ}$. For this experiments $_{81}$Tl was chosen. It has hexagonal (hpc) structure for temperatures below 503 K and a cubic (bcc) structure for temperatures above it. The EFG of Tl is strongly temperature dependent and decreases with temperature. The experiment was carried at $T = 473(1)$ K, providing an optimal EFG for the experiment. The EFG selection is based on theoretical calculations within the density-functional theory, using the full-potential linearized augmented plane wave (LAPW) method as implemented in the WIEN97 package [41] and the measured temperature dependence of the EFG, which follows the $T^{3/2}$ low [42]. The calculation yields a value of V_{ZZ}(WTl) = $2.54 \cdot 10^{21}$ V/m^2 at 0 K, which is derived from the self-consistent charge density without further approximations. A theoretical uncertainty of 10% for the LAPW calculation is taken into consideration. A dedicated experiment to measure the temperature dependence factor was performed and a value $b = 7.6 \left(^{+0.2}_{-0.4}\right) \cdot 10^{-5}$ K$^{-3/2}$ was derived, resulting in a value V_{ZZ}(WTl) = $0.55 \left(^{+0.12}_{-0.08}\right) \cdot 10^{21}$ V/m^2 at 473 K.

The Tl host was heated above 503 K during the experiments which allows the full anisotropy of the γ rays to be measured directly. In this case no EFG is present and the initial orientation of the spin ensemble is kept over the whole field range. This allows the conclusion that decoupling is achieved in the experiment and is a direct prove for the proper choice of the magnitude of the EFG for the LEMS experiment.

A quadrupole frequency $\nu_Q = 53(8)$ MHz was measured and the spectroscopic quadrupole moment of the $K = \frac{35}{2}$ isomer in ^{179}W was found to be $Q_s = 4.00 \left(^{+0.83}_{-1.06}\right)$ eb. Accepting that K is a good quantum number, the intrinsic quadrupole moment can be derived through the relation:

$$Q_s = Q_0 \frac{3K^2 - I(I+1)}{(2I+3)(I+1)}. \tag{2}$$

This yields a value $Q_0 = 4.73 \left(^{+0.93}_{-1.06}\right)$ eb, which corresponds to a quadrupole deformation $\beta_2 = 0.185 \left(^{+.0038}_{-0.049}\right)$. In the Figure 4 the systematic theoretical predictions for the ground-state deformations for the $_{74}$W nuclei are compared to values obtained from $B(E2)$ measurements [43] and to the derived deformation of the $K = \frac{35}{2}$ isomer in ^{179}W. The calculations yield similar deformations for the

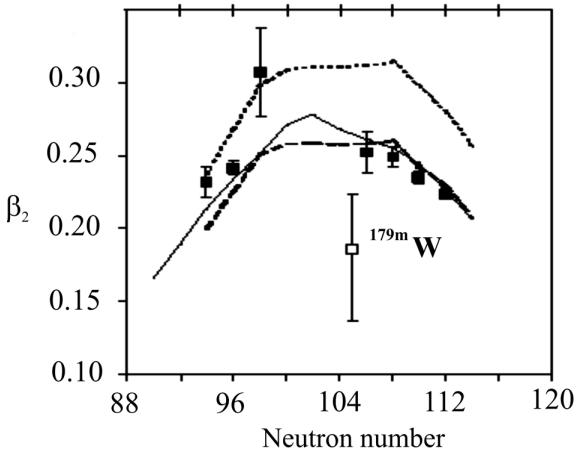

Figure **4.** The deduced quadrupole deformation for the $K = \frac{35}{2}$ isomer in ^{179}W (open square) is compared to different theoretical calculations of ground-state deformations and deformations deduced from $B(E2)$ experimental data.

ground-state and the five-quasiparticle K isomer, while the experimental value for the isomer is about one σ away from the ground-state systematics. Similar difference was observed also for ^{182}Os (if equal mean-sqare radii are considered for both excitations), while ^{177}Lu and ^{178}Hf the K isomer and the ground state have similar deformations.

5 Summary

Several recent experiments related to investigations of static quadrupole moments or $B(E2)$ strength are reported. The derived $B(E2)$ reduced transition probabilities in the ground-state band of ^{128}Ce indicate that this nucleus lies close to the U(5)-SU(3) phase shape transition and it is suggested as a benchmark for the X(5) critical point symmetry in the mass $A \approx 130$ region. A comparison with other valence mirror nuclei in the N_pN_n scheme poses the question on the role of particle states for critical-point behavior. The measurements of the band-head static quadrupole moment and lifetimes in the yrast three-quasiparticle magnetic band in ^{193}Pb demonstrate that this state has moderate oblate deformation, which is determined by the 2p2h excitations across the $Z = 82$ shell, The measured complete set of experimental observables provides a test ground for theoretical models. The measurement of the quadrupole moment of the $K = \frac{35}{2}$ five-quasiparticle, high-K isomer ^{179}W yields smaller deformation for this state compared to the systematics of the ground-state deformations in the $_{75}$W nuclei. All results help the detailed understanding of these excitations and put constrains of the theoretical models aiming at their description.

Acknowledgments

This work was supported in part by the EC EURONS RII3-CT-2004-506065 project, the Bulgarian National Science Fund under grant VUF06/05 and the Yale Flint and Scientific Development Fund.

References

1. F. Iachello, N.V. Zamfir, *Phys. Rev. Lett.* **92**, 212501 (2004).
2. D.L. Balabanski *et al.* (2006) *Proc. Int. Conf. on Nuclear Structure, Shanghai, 2006* eds. Y.M. Zhao *et al. Int. J. Mod. Phys. E* in print.
3. D.L. Balabanski *et al.*, *Eur. Phys. J. A* **20**, 191 (2004).
4. D.L. Balabanski *et al.*, *Phys. Rev. Lett.* **86**, 604 (2001).
5. K.A. Gladnishki *et al.*, *J. Phys. G* **31**, S1559 (2005).
6. F. Iachello, *Phys. Rev. Lett.* **85**, 3580 (2000).
7. F. Iachello, *Phys. Rev. Lett.* **87**, 052502 (2001).
8. F. Iachello, A. Arima, *The Interacting Boson Model* (Cambridge Univ. Press, 1987).
9. R.F. Casten, N.V. Zamfir, *Phys. Rev. Lett.* **85**, 3584 (2000).
10. R.F. Casten, N.V. Zamfir, *Phys. Rev. Lett.* **87**, 052503 (2001).
11. A. Bohr, *Mat. Fys. Medd. K. Dan. Vidensk. Selsk.* **36**, no. 14 (1952).
12. A. Dewald *et al.*, *Z. Phys. A* **334**, 163 (1989).
13. G. Winter, *Nucl. Instr. and Meth.* **214**, 537 (1983).
14. G. Böhm *et al.*, *Nucl. Instr. and Meth. A* **329**, 248 (1993).
15. P. Petkov *et al.*, *Nucl. Phys. A* **640**, 293 (1998).
16. J.C. Wells *et al.*, *Phys. Rev. C* **30**, 1532 (1984).
17. J.R. Cooper, *Ph.D. Thesis* (Yale University, New Haven, 2002).
18. G.S. Li *et al.*, *Z. Phys. A* **356**, 119 (1996).
19. P.G. Bizzeti, A.M. Bizzeti-Sona, *Phys. Rev. C* **66**, 031301 (2002).
20. C. Hutter *et al.*, *Phys. Rev. C* **67**, 054315 (2003).
21. R. Bijker *et al.*, *Phys. Rev. C* **68**, 064304 (2003); erratum: *ibid* **C69**, 059901 (2004).
22. H. Hubel, *Prog. Part. Nucl. Phys.* **28**, 427 (1992); *ibid* **54**, 1 (2005).
23. R. Clark, A.O. Machiavelli, *Annu. Rev. Nucl. Part. Sci.* **50**, 1 (2000).
24. A. Bohr, B.R. Mottelson, *Nuclear Structure vol. II* (Benjamin, New York, 1975).
25. Amita, A.K. Jain, B. Singh, *At. Data Nucl. Data Tables* **74**, 283 (2000).
26. M. Ionescu-Bujor *et al.*, *Phys. Rev. C* **70**, 034305 (2004).
27. K. Vyvey, D.L. Balabanski, G. Neyens, *Eur. Phys. J. A* **22 s01**, 1 (2004).
28. G. Baldseifen *et al.*, *Phys. Rev. C* **54**, 1106 (1996).
29. L. Ducroux *et al.*, *Z. Phys. A* **356**, 241 (1996).
30. S. Chmel *et al.*, *Phys. Rev. Lett.* **79**, 2002 (1997).
31. S. Frauendorf, *Rev. Modern Phys.* **73**, 462 (2001).
32. S. Chmel, *Ph.D. Thesis* (University of Bonn, 2005) and private communication.
33. P.M. Walker, G.D. Dracoulis, *Nature (London)* **399**, 35 (1999).
34. C. Broude *et al.*, *Phys. Lett.* **264b**, 17 (1991).
35. N. Boss *et al.*, *Phys. Rev. Lett.* **72**, 2689 (1994).
36. E. Lubkiewicz *et al.*, *Z. Phys. A* **355**, 377 (1996).
37. U. Georg *et al.* (1998) *Eur. Phys. J. A* **3** 225.
38. J. Billowes *et al.*, *Nucl. Phys. A* **752**, 309c (2005) and the references therein.

39. R. Coussement *et al.*, *Hyperfine Interact.* **23**, 273 (1985).
40. F. Hardeman *et al.*, *Phys. Rev. C* **43**, 130 (1991).
41. P. Blaha *et al.*, *WIEN97 ISBN 3-9501031-0-4* (Technological Univ. Vienna, 1997).
42. G. Schatz *et al.*, *Z. Phys. B* **49**, 23 (1982).
43. S. Raman *et al.*, *At. Data Nucl. Data Tables* **36**, 1 (1987); *ibid* **42**, 1 (1989).